

Injection fluid selection based on equation of state for numerical simulation of miscible condensate displacement

Wybór płynu zatłaczanego w oparciu o równanie stanu do symulacji numerycznej wypierania rozpuszczalnego kondensatu

Oleh Lukin, Oleksandr Kondrat

Ivano-Frankivsk National Technical University of Oil and Gas

ABSTRACT: Condensate dropout in the reservoir, below the saturation pressure, leads to a change in the composition of hydrocarbon gas and liquid at reservoir conditions, blocking part of the pore space, resulting in reduced well productivity. It also causes the composition of the fluid carried to the surface to contain a smaller amount of valuable intermediate hydrocarbon components such as C5+. The condensate dropped-out in the reservoir remains immobile until its saturation exceeds the critical saturation, or it is re-evaporated by miscible injection at pressure. The volume of the condensate bank in the reservoir and the resulting residual condensate reserves can reach tens of millions of m³ and, as a rule, consist of light and valuable hydrocarbon fractions. This publication investigates, using a compositional hydrodynamic simulator, the possibility of re-vaporizing a given volume of condensate and producing it by injecting a fluid that, at a given pressure and temperature, will mix with the condensate in the reservoir and form a single phase. A low-permeability gas condensate reservoir (0.001–0.1 mD), developed using a horizontal well with multi-stage hydraulic fracturing, is considered as a synthetic model. The results of the simulation showed a significant change in the composition of reservoir fluids with a corresponding decrease in reservoir pressure. The composition of the dropped-out condensate was determined, and a method for its mobilization by sequential injection of a mixing agent and production (huff-and-puff) was tested for different injection fluids. The methodology for selecting an injection agent based on the equation of state (EOS) in a PVT package for mixing displacement is considered and described. This type of numerical sensitivity provides a better understanding of the phase behavior of gas condensate, not only along the wellbore or fractures but also deep into the reservoir. It allows engineers to better optimize the development process and achieve significantly higher gas and condensate recovery rates by injecting a miscible fluid that is properly selected for a particular fluid system.

Key words: condensate miscibility, equation of state, hydrodynamic simulation, tight gas.

STRESZCZENIE: Wytrącanie kondensatu w złożu poniżej ciśnienia nasycenia prowadzi do zmiany składu węglowodorów gazowych i ciekłych w warunkach złożowych, blokując część przestrzeni porowej, co skutkuje zmniejszoną produktywnością odwiertu. Powoduje to również, że skład płynu wynoszonego na powierzchnię zawiera mniejszą ilość cennych pośrednich składników węglowodorowych, takich jak C5+. Wytrącony w złożu kondensat pozostaje nieruchomy do momentu, aż jego nasycenie przekroczy nasycenie krytyczne lub zostanie ponownie odparowany w wyniku zatłaczania mieszalnego płynu pod odpowiednim ciśnieniem. Objętość kondensatu zalegającego w złożu i wynikające z tego rezydualne zasoby kondensatu mogą sięgać dziesiątek milionów m³ i z reguły składają się z lekkich i cennych frakcji węglowodorowych. W niniejszej publikacji zbadano, przy użyciu kompozycyjnego symulatora hydrodynamicznego, możliwość ponownego odparowania danej objętości kondensatu i jego wydobywania poprzez zatłaczanie płynu, który przy danym ciśnieniu i temperaturze zmiesza się z kondensatem w złożu, tworząc jedną fazę. Jako model syntetyczny rozważono złożę gazu kondensatowego o niskiej przepuszczalności (0,001–0,1 mD), eksploatowane za pomocą poziomego odwiertu z wielostopniowym szczelinowaniem hydraulicznym. Wyniki symulacji wykazały znaczną zmianę składu płynów złożowych wraz z odpowiadającym jej spadkiem ciśnienia złożowego. Określono skład wytrąconego kondensatu oraz przetestowano metodę jego mobilizacji poprzez sekwencyjne zatłaczanie środka mieszającego i wydobywanie (metoda *huff-and-puff*) dla różnych płynów zatłaczanych. Rozważono i opisano metodologię doboru czynnika zatłaczanego w oparciu o równanie stanu (EOS) w pakiecie PVT dla wypierania mieszalnego. Tego rodzaju analiza numeryczna pozwala lepiej zrozumieć zachowanie fazowe gazu kondensatowego nie tylko wzdłuż otworu wiertniczego czy szczelin, ale również głęboko w złożu. Umożliwia to inżynierom lepszą optymalizację procesu eksploatacji i osiągnięcie znacznie wyższych współczynników odzysku gazu i kondensatu poprzez zatłaczanie odpowiednio dobranego, mieszalnego płynu dla danego układu złożowego.

Słowa kluczowe: rozpuszczalność kondensatu, równanie stanu, symulacja hydrodynamiczna, gaz zamknięty.

Introduction

Condensate banking and its impact on well productivity is one of the major problems in the development of low-permeability gas condensate reservoirs, especially when the initial reservoir pressure and saturation pressure are close, and the reservoir fluid is characterized by a high condensate gas ratio (CGR). According to Pope et al. (2000), this is due to the formation of a two-phase flow in the reservoir, which significantly reduces the relative permeability of gas in the presence of liquid. The standard procedure for minimizing condensate drop-out in the reservoir is multi-stage hydraulic fracturing. However, in low-permeability reservoirs, a decrease in reservoir pressure along horizontal wells can cause a drop in well productivity over time, also due to the formation of a condensate ring. Bang et al. (2008) pointed out that condensate blockage occurring along fractures, resulting from hydraulic fracturing, also significantly reduces well productivity. Many studies have been carried out to minimize condensate deposition in the reservoir by gas injection, to maintain reservoir pressure above saturation pressure, to vaporize an already formed condensate bank, or to use various types of solvents such as methanol (MeOH) or iso-propanol (IPA). In this study, the focus is on optimizing the methodology for selecting gas for injection, based on the tuned equation of state and composition of the condensate to achieve miscible displacement in the reservoir.

Al Kharusi et al. (2019) considered various enhanced recovery methods for a depleted gas condensate field, where the effect of CO₂, N₂, and dry gas injection on additional condensate recovery was hydrodynamically investigated. The results showed that as the volume of CO₂ injection increased, the cumulative production of condensate also increased, but the limited availability of CO₂ and the relatively distant location of its source were highlighted as major bottlenecks. Dry gas injection required significant injection pressure and volume. Recirculating 100% of the produced gas back into the reservoir increased condensate production, according to the model, but required freezing a significant amount of hydrocarbon gas, which was currently impossible to sell to neighboring markets. The injection of N₂ had a negative impact and only increased the amount of liquid phase in the reservoir. It should be noted that in this study, the selection of fluid for injection was performed at the simulation stage by applying various injection streams. Burachok et al. (2021) considered, using a synthetic model, the possibility of employing various EOR methods to increase the recovery of gas and condensate from deep reservoirs in the Dnieper-Donets Rift (Ukraine). The following injection mixtures were considered: 1) 100% CO₂; 2) 90% C₁, 5% C₂, 5% C₃; 3) 98% C₁, 1% C₂, 1% C₃; 4) 50% C₁, 50% N₂ and others. In this case, the highest condensate recovery

was achieved during the injection of 100% CO₂, while from an economic point of view, 100% C₁ was the best injection agent. The authors also recommend starting gas injection before the reservoir pressure drops to saturation pressure. In this case, condensate production is maximized. Rivero et al. (2019) studied gas injection into low-permeability gas condensate reservoirs in combination with multi-stage hydraulic fracturing under different parameters. A sensitivity analysis was carried out to study the combined effect of changes in the distance between the stages of hydraulic fracturing, their configuration, and gas injection of the following compositions: 1) 100% C₁; 2) 75% C₁, 25% C₂ and 3) 70% C₁, 15% C₂, 15% C₃. However, the authors of the above publications test the effect of various injection agents at the level of a hydrodynamic simulator of the compositional type. This article aims to unify an alternative method for selecting the optimal injection fluid by determining the minimum required miscibility pressure and the potential for re-vaporization of the condensate dropped-out in the reservoir in order to form a single-phase flow.

The relevance of this topic lies in the possibility of assessing the composition of the condensate in different parts of the reservoir using a hydrodynamic simulator and selecting a mixing agent for the re-vaporization of this volume of hydrocarbons and miscible displacement, ultimately leading to increased production.

Theoretical review

Understanding the composition (by components) of condensate and its properties is critical for the design of miscible injection and agent selection to increase the mobilization of a given volume of liquid into development/production. One of the main advantages of compositional modeling is the ability to determine the % mol of each component included in the equation of state, in both gaseous and liquid states, in any part of the reservoir under various pressure conditions over time. To mobilize the condensate that has dropped out in the reservoir, various schemes of gas recirculation or injection of various types of agents are used for its further vaporization or mixing. Successful design and implementation of such development schemes require accurate prediction and understanding of compositional effects that control the effectiveness of local displacement through miscibility. Miscibility is the property of a substance to mix in all proportions, thereby forming a homogeneous (single-phase) fluid. This property is associated with surface tension: if it is zero, then the fluids are mutually soluble. In the case of gas injection, the resulting mixture in the reservoir can form either a single phase or two separate phases (liquid and gas). If the mixture is in a single-phase,

miscible displacement occurs; otherwise, the mixing process does not occur. According to Stalkup (1983), gas injection into gas condensate reservoirs to achieve a single-phase flow by vaporization and mixing of the precipitated condensate with gas has been applied in many fields around the world.

Several authors have investigated the use of gas injection as a method of increasing condensate recovery. According to Seteyeobot et al. (2021), there are three main methods of gas injection: intermittent, continuous, and cyclic. Using these methods, improvements in the development schemes for depleted gas condensate fields were presented by Ghiri et al. (2015) and Hamdi et al. (2020). They demonstrated an increase in the condensate recovery rates and a decrease in residual condensate saturation along the displacement front during gas injection. It should be noted that miscibility can be achieved with both hydrocarbon and non-hydrocarbon gases, as demonstrated by Mohammed et al. (2020) during experimental studies with alternating injection of N₂ and CO₂.

To assess the miscibility of the condensate dropped-out in the reservoir with hydrocarbon or non-hydrocarbon gas of a certain composition, laboratory studies are carried out and compared with the previously tuned equation of state. For this purpose, the ternary diagram or Gibbs triangle of Weisstein (2021) is used. It is a barycentric graph of three variables whose sum is equal to a constant. A ternary diagram graphically depicts the relationship of three variables as positions in an equilateral triangle. In such a graph, the sum of the three variables must be equal to some constant (for example, A + B + C). Usually, this constant is 100%. This is an alternative method for visualizing the boundary of single- and two-phase flow regions. The diagram represents a snapshot of certain reservoir conditions and is constructed at a constant pressure and temperature, while fluid composition is a variable. A ternary diagram, like

a phase diagram, shows the size and shape of a two-phase region. However, while a phase diagram has a constant composition and is a function of pressure and temperature, a ternary diagram, at constant pressure and temperature, is a function of composition. Multicomponent fluids can be represented on ternary diagrams by conditionally grouping the N-component system into three groups (pseudo-ternary diagrams):

- the light group contains components C1 and N₂,
- the middle group contains CO₂, H₂S and hydrocarbon components from C2 to C6,
- the heavy group consists of all C7+ components.

Figure 1 represents an empty ternary diagram (1) and the intersection method showing how to read the ternary diagrams (2).

The detailed form of a ternary diagram also depends on how components are grouped. However, the light group is always placed at the top of the triangle, the middle group at the bottom right, and the heavy group at the bottom left. While there are no standardized names for these groups, for simplicity, we denote the light group as (1), the medium group as (2), and the heavy group as (3). The phase diagram within the triangle separates the single- and two-phase regions. Similar to a phase envelope, the ternary diagram includes dew point lines, bubble point lines, and a critical point, as presented in Figure 2.

The line where the gas bubble first appears is equivalent to the bubble point line and is usually located on the left side of the triangle, and the line where the first drop of liquid appears is the dew point line and is on the right side of the triangle. Since dropped-out condensate in the reservoir is characterized by heavy hydrocarbon components of significant value, researchers focus primarily on their properties and the possibility of mobilizing them in the reservoir for further production. The point where the dew point line and bubble point line connect is the critical point, analogous to the critical point in a phase diagram.

Figure 3 shows the key elements of the ternary diagram: 1 – bubble point line, 2 – dew point line, 3 – critical point, 4 – two-phase region, 5 – single-phase region, 6 – projection of the critical point.

Line 6 is critical when visually assessing the miscibility of the different fluids represented in the ternary diagram. It should be noted that the size and shape of the two-phase region visualized in the diagram will vary depending on pressure and temperature. As reservoir pressure increases, the size of the two-phase region will decrease. Similarly, it decreases with

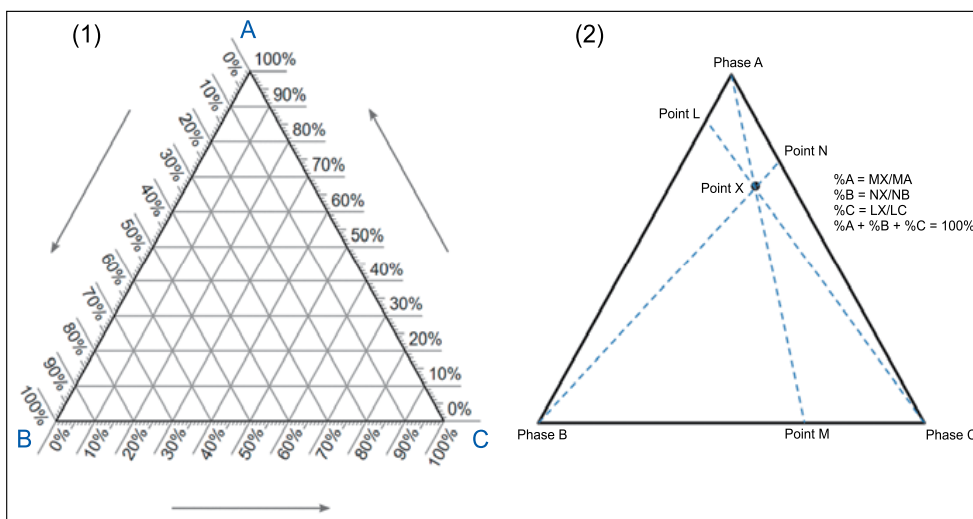


Figure 1. Empty ternary diagram and intersection method

Rysunek 1. Pusty diagram trójskładnikowy i metoda intersekcyjna

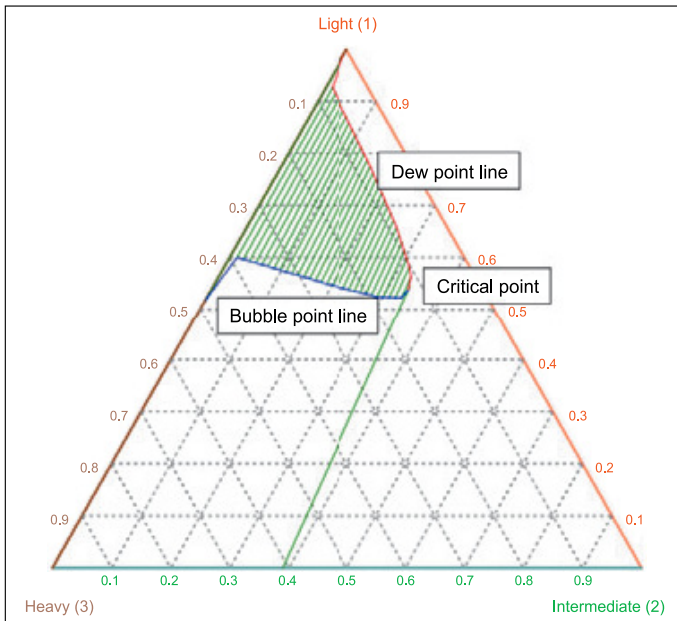


Figure 2. Typical ternary diagram and its elements

Rysunek 2. Typowy diagram trójskładnikowy i jego elementy

an increase in reservoir temperature. Also, depending on the composition and grouping, the ternary diagram can display the fluid of a certain composition as a point. Figure 4 shows an example of a constructed ternary diagram at different values of reservoir pressure.

In the case of immiscible fluids, the mobility of each phase is determined by the relative permeability. At the same time, during mixing, a single phase is formed, whose mobility is higher because the influence of the phase permeability is almost absent. From the perspective of hydrodynamic simulation, the main advantage of phase solubility is the absence or near-zero residual saturation during displacement. For a given reservoir temperature, miscibility depends on pressure and composition. This introduces the concept of the minimum miscibility pressure

(MMP). In theory, first-contact miscibility can be achieved for most gases; however, the pressure required is extremely high. From a practical point of view, reservoir pressure or bottom-hole injection well pressure cannot reach such values. Therefore, a distinction is made between miscibility at first contact and multi-contact miscibility, which are characterized by the minimum required mixing pressures at the first or multiple contacts.

At a given pressure and temperature, first contact miscibility means that the two fluids are mutually soluble at any concentration, and the resulting mixture always remains the same single phase. From the point of view of the ternary diagram, first-contact miscibility can be achieved at a given pressure and temperature if a line (A) can be drawn between the initial

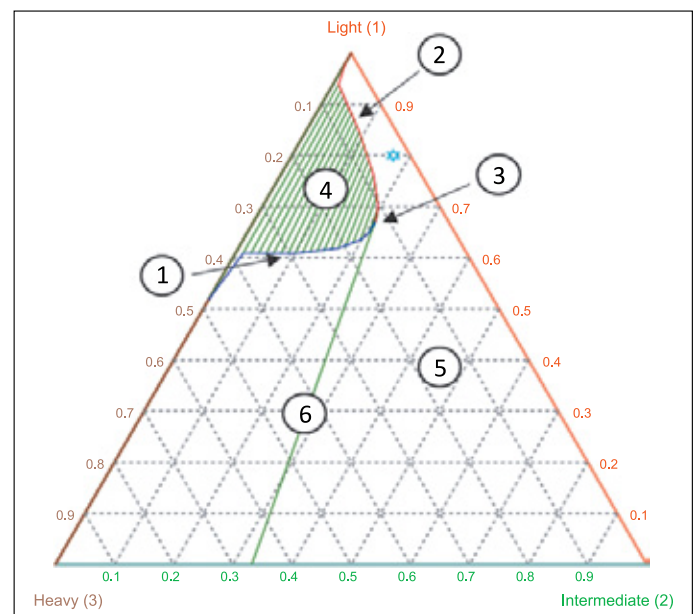


Figure 3. Ternary diagram for tuned EOS at reservoir pressure of 250 bar and reservoir temperature of 80°C

Rysunek 3. Diagram trójskładnikowy dla dopasowanego równania stanu przy ciśnieniu złożowym 250 barów i temperaturze złoża 80°C

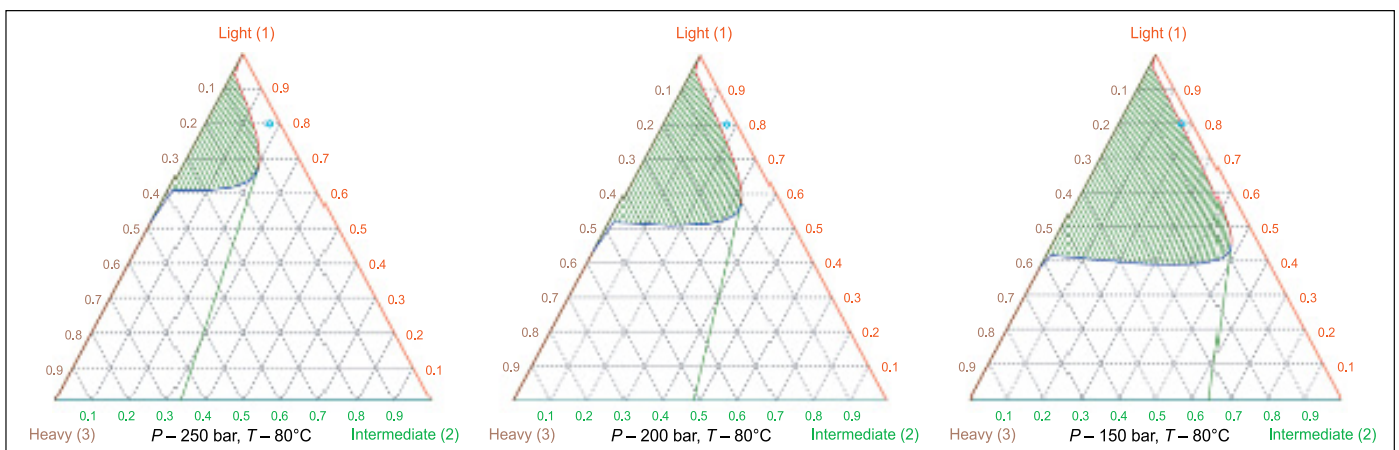


Figure 4. Ternary diagram example for tuned EOS at reservoir pressure of 250 bar and reservoir temperature of 80°C

Rysunek 4. Przykładowe diagramy trójskładnikowe dla dopasowanego równania stanu przy ciśnieniu złożowym 250 barów i temperaturze złoża 80°C

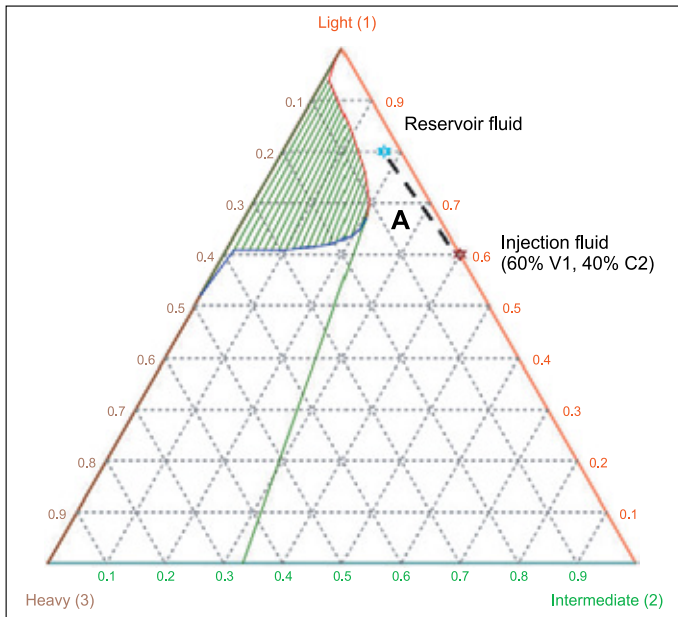


Figure 5. Ternary diagram for tuned EOS at reservoir pressure of 250 bar and reservoir temperature of 80°C with injection of 60% C1, 40% C2

Rysunek 2. Diagram trójskładnikowy dla dopasowanego równania stanu przy ciśnieniu złożowym 250 barów i temperaturze złoża 80°C oraz przy zatłaczaniu 60% C1, 40% C2

fluid and the fluid to be injected without crossing the two-phase region or the critical point projection as shown in Figure 5.

Mixing at first contact will not always be possible for several reasons, such as:

- reservoir pressure is higher than the minimum miscibility pressure;
- a higher concentration of solvent is required, which increases costs;
- distance from the two-phase region.

Therefore, in practice, multi-contact mixing of fluids serves as an alternative. Miscibility occurs over multiple contacts, and it is a complex, dynamic process that depends numerous unknown and local compositional changes in the reservoir, which cannot always be determined with the necessary precision using a PVT cell. When injecting gas containing hydrocarbon components such as C2, C3, C4 or solvents, as the saturation of these components increases, the

condensate adsorbs part of them. Thus, the resulting mixture becomes lighter until the saturation reaches critical values, and a lighter single-phase fluid is formed – miscibility is achieved. However, this process depends on the composition of the reservoir fluid (dropped-out condensate), the composition of the injected fluid, and reservoir conditions (pressure and temperature). Thus, miscibility cannot always be achieved. From the perspective of the ternary diagram, if the reservoir fluid and the injected fluid are on opposite sides of the critical point projection and the two-phase region (at a given pressure and temperature), first-contact miscibility is not possible, as shown in Figure 6.

In cases where the saturation of the injected fluid increases, the composition of the liquid changes from L_1 to L_2 , and the gas composition from V_1 to V_2 . As a result, a new mixture of M_1 and M_2 is formed. This process continues until saturation with the injected fluid reaches a critical value and miscibility is achieved.

Figure 7 shows an example of the process of reservoir fluid enrichment, showing how composition changes to approach the critical point and achieve miscibility.

If we extend the critical point projection and draw a tangent from the point representing the composition of the condensate dropped-out in the reservoir, we can distinguish three regions (compositions) of the injected gas, as illustrated in Figure 8:

1. composition of a gas for which miscibility cannot be achieved;
2. gas composition with multi-contact miscibility;
3. gas composition with first contact miscibility;
4. tangent line from the composition of the dropped-out condensate.

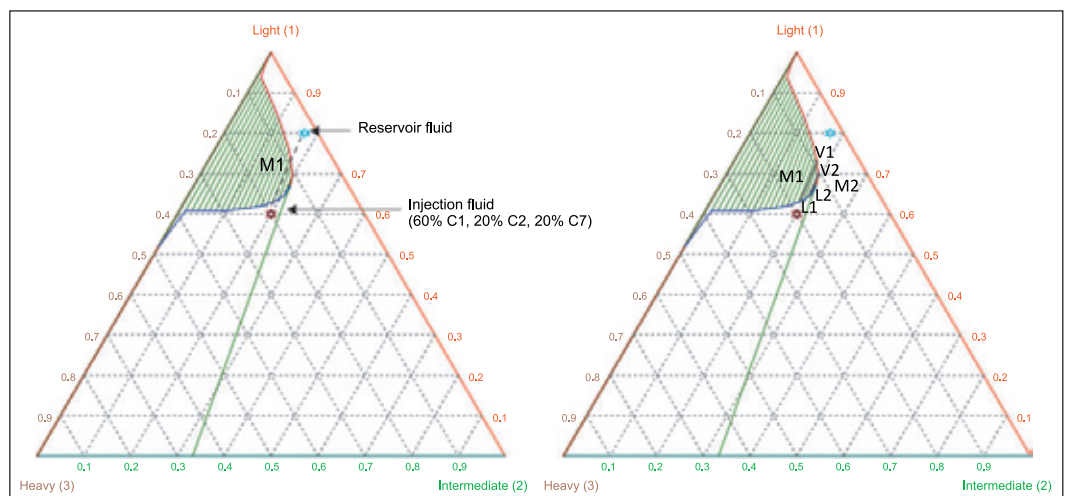


Figure 6. Ternary diagram for tuned EOS at reservoir pressure of 250 bar and reservoir temperature of 80°C with injection of 60% C1, 20% C2, 20% C7

Rysunek 6. Diagram trójskładnikowy dla dopasowanego równania stanu przy ciśnieniu złożowym 250 barów i temperaturze złoża 80°C oraz przy zatłaczaniu 60% C1, 20% C2, 20% C7

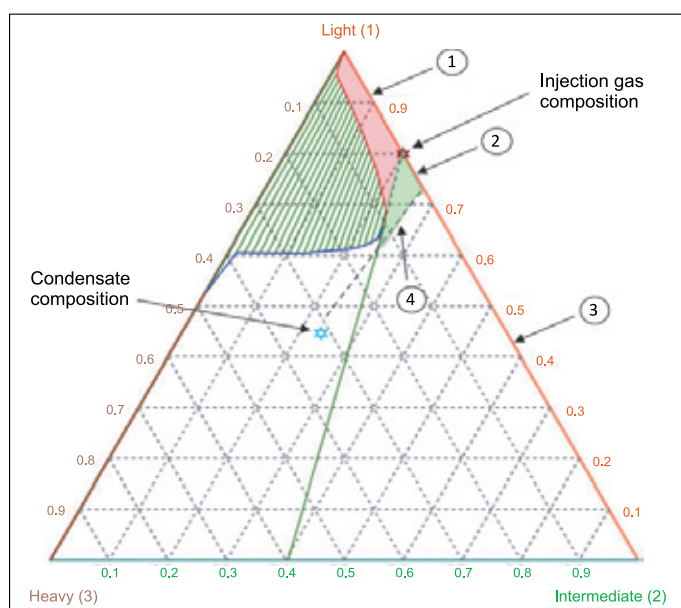


Figure 7. Ternary diagram with critical point extension and tangent to define composition of miscible gas injection

Rysunek 7. Diagram trójskładnikowy z przedłużeniem punktu krytycznego i styczną w celu określenia składu zatłoczonego gazu mieszalnego

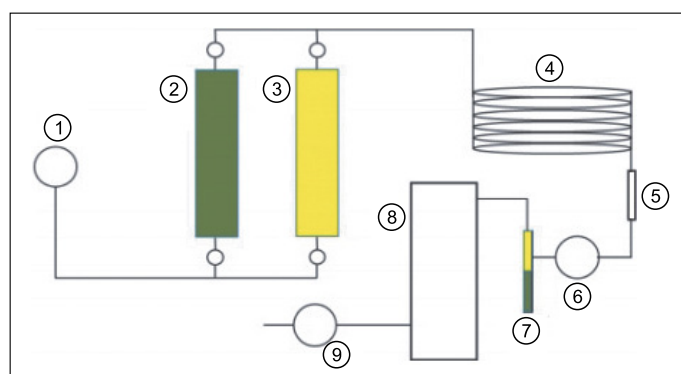


Figure 8. Slim tube experiment scheme: 1 – pump; 2 – oil/condensate tank; 3 – injection gas; 4 – twisted tube; 5 – sight glass; 6 – pressure regulator; 7 – separator; 8 – chromatograph; 9 – gasometer

Rysunek 8. Schemat eksperymentu z cieniłą rurką: 1 – pompa; 2 – zbiornik oleju/kondensatu; 3 – gaz wtryskowy; 4 – skręcona rurka; 5 – wziernik; 6 – regulator ciśnienia; 7 – separator; 8 – chromatograf; 9 – gazometr

If reservoir pressure or injection pressure is lower than the minimum miscibility pressure, the solvent and the condensate dropped in the reservoir are not mutually soluble. However, as contact between the phases increases (increasing the saturation of the gas phase – the solvent), the mixture in the reservoir will change its composition until miscibility is achieved. Thus, with the help of a ternary diagram, it is possible to determine the feasibility of injecting an agent of a certain composition to mobilize part of condensate volume that has dropped in the reservoir. To assess the quantitative and qualitative character-

istics of this process more thoroughly in laboratory conditions, an additional slim tube experiment is carried out, based on which the equation of state is also calibrated. This experiment is conducted to determine the minimum pressure for multi-contact miscibility. The essence of the experiment is to inject gas (solvent) of a certain composition into oil (condensate) at different pressures. Figures 8–9 show the scheme of the experiment and the graphical determination of the minimum miscibility pressure. The oil/condensate production obtained during the experiment is visualized as a function of pressure. 1 – zone of immiscible displacement; 2 – multi-contact miscibility; 3 – minimum miscibility pressure.

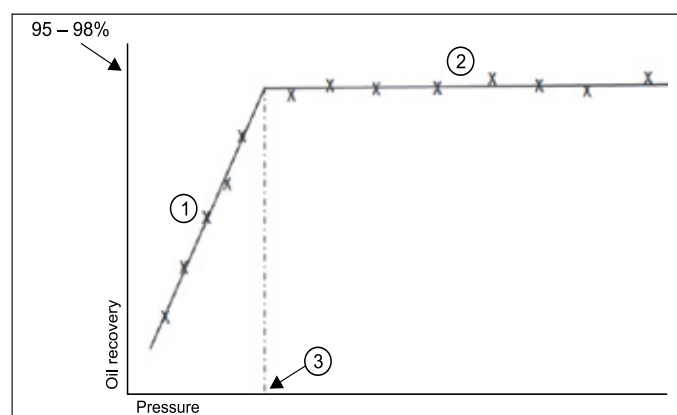


Figure 9. Idealized oil/condensate extraction during slim tube experiment

Rysunek 9. Modelowy proces ekstrakcji ropy/kondensatu podczas eksperymentu z cieniłą rurką

Therefore, as reservoir pressure increases, the size of the two-phase region in the ternary diagram decreases until miscibility is achieved. At the same time, the pressure values and the condensate recovery coefficient will be maximized since the condensate and gas form a single phase. The residual condensate saturation is reduced to minimum values at the minimum multi-contact miscibility pressure. However, even in laboratory conditions, it is difficult to accurately determine the minimum miscibility pressure, so this parameter will always be characterized by a certain uncertainty.

To mobilize a given volume of condensate, the injection of a miscible agent is typically used. Injection can be performed through vertical injection wells drilled along the contour of the intended condensate bank. However, in low-permeability reservoirs, the injectivity capacity of these wells, even after hydraulic fracturing, may be low and may not reach the required injection volume or miscibility pressure. As a pilot project, a producing horizontal well with a specific completion can be used. This approach allows for cyclic injection of the agent to achieve vaporization of the condensate and subsequent production (huff-and-puff method).

Results and discussions

Equation of state modeling

The following tuned equation of state for the gas condensate reservoir allows not only the determination of the composition of the liquid and gaseous phases at different reservoir pressure values but also the calculation of their properties. The research area is characterized by 3 surface samples for gas and liquid. Physical recombination was performed for the PVT lab experiments.

The Peng-Robinson equation is used as the equation of state, and the viscosity model is calculated using the empirical Lohrenz-Bray-Clark correlation. The following correlations are used to determine the parameters of the equation of state:

- critical temperature (T_c) – Kesler – Lee;
- critical pressure (P_c) – Kesler – Lee;
- acentric factor (ω) – Kesler – Lee.

The resulting phase envelope for the tuned EOS is shown in Figure 10. Reservoir fluid composition and component proper-

ties are summarized in Table 1. The reservoir temperature is 80°C, and the saturation pressure is 261 bar. The equation of state is represented by a set of parameters for each component, representing the reservoir fluid.

Constant composition expansion (CCE) was performed for a recombined sample at a maximum pressure of 5511 psi (380 bar) and minimum pressure of 290 psi (20 bar) at a reservoir temperature of 80°C. The resulting saturation pressure is 218 bar. Constant volume depletion (CVD) was conducted at a saturation pressure of 3780 psi (218 bar) down to a minimum pressure of 290 psi (20 bar). The dropped-out liquid volume, cumulative liquid production, and Z-factors were measured at each pressure depletion step. Additionally, the fluid composition was determined at key pressure steps. The Fluid Modeler PVT package was used for all equation of state modeling work. Calibrated laboratory experiments vs observed data are presented in Figures 11–12.

Physical parameters of the condensate were determined at different reservoir pressure values. In this case, the density of the dropped-out condensate changed from 612 kg/m³ ($P = 215$ bar) to 659 kg/m³ ($P = 70$ bar). The viscosity under the same conditions changed from 0.201 to 0.254 cP. An increase in the molar percentage of heavy fractions directly affects the density and viscosity of the liquid under reservoir conditions. Therefore, the calibration of the equation of state should not only be performed according to the properties of the fluids, but also the phase changes (% mol component) should be reproduced at each pressure value below the saturation pressure. The calibrated equation of state was used to estimate the composition of the resulting condensate ring based on the results of the CCE experiment in the PVT package. The condensate composition is then used to estimate the minimum

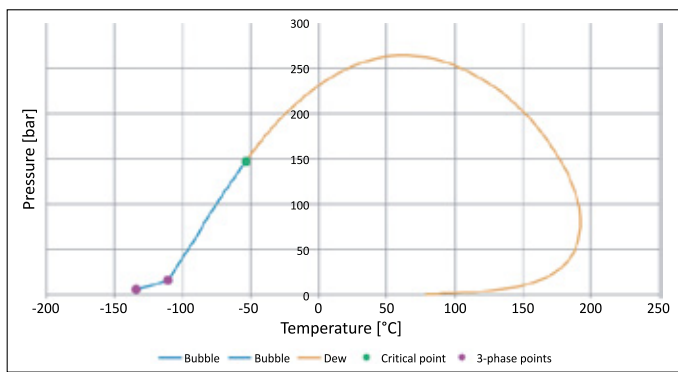


Figure 10. Phase envelope for tuned equation of state (EOS)
 Rysunek 10. Wykres fazowy dla dostosowanego równania stanu

Table 1. Reservoir fluid composition and component properties
 Tabela 1. Skład płynu złożowego i właściwości jego składników

Component	Molecular weight	Spec. gravity	Mole [%]	Mass [%]	Boiling point [°C]	Critical temperature [°C]	Critical pressure [bar]	Acentric factor	Critical volume [m ³ /mol]	Volume translation
	[g/mole]									
N ₂	28.01		0.87	0.83	77.40	126.20	33.94	0.04	0.00009	-0.13
CO ₂	44.01		0.25	0.38	194.70	304.70	73.87	0.23	0.00009	-0.04
C1	16.04		74.52	40.83	111.60	190.60	46.04	0.01	0.00010	-0.14
C2	30.07		10.16	10.43	184.60	305.43	48.84	0.10	0.00015	-0.10
C3	44.10		4.07	6.13	231.10	369.80	42.46	0.15	0.00020	-0.08
i-C4–n-C5	62.82	0.59	2.60	5.58	280.94	434.62	36.23	0.21	0.00028	-0.05
C7–C8	95.13	0.72	2.45	7.96	363.10	538.75	31.14	0.31	0.00039	-0.01
C9–C10	122.49	0.77	2.20	9.20	420.27	605.21	27.98	0.40	0.00049	0.00
C11–C14	162.21	0.80	1.77	9.81	482.10	663.33	21.77	0.53	0.00064	0.07
C15–C19	225.27	0.84	0.99	7.62	559.60	558.33	17.83	0.68	0.00084	0.09
C20+	300.00	0.86	0.12	1.23	658.60	773.11	13.17	0.95	0.00120	0.25

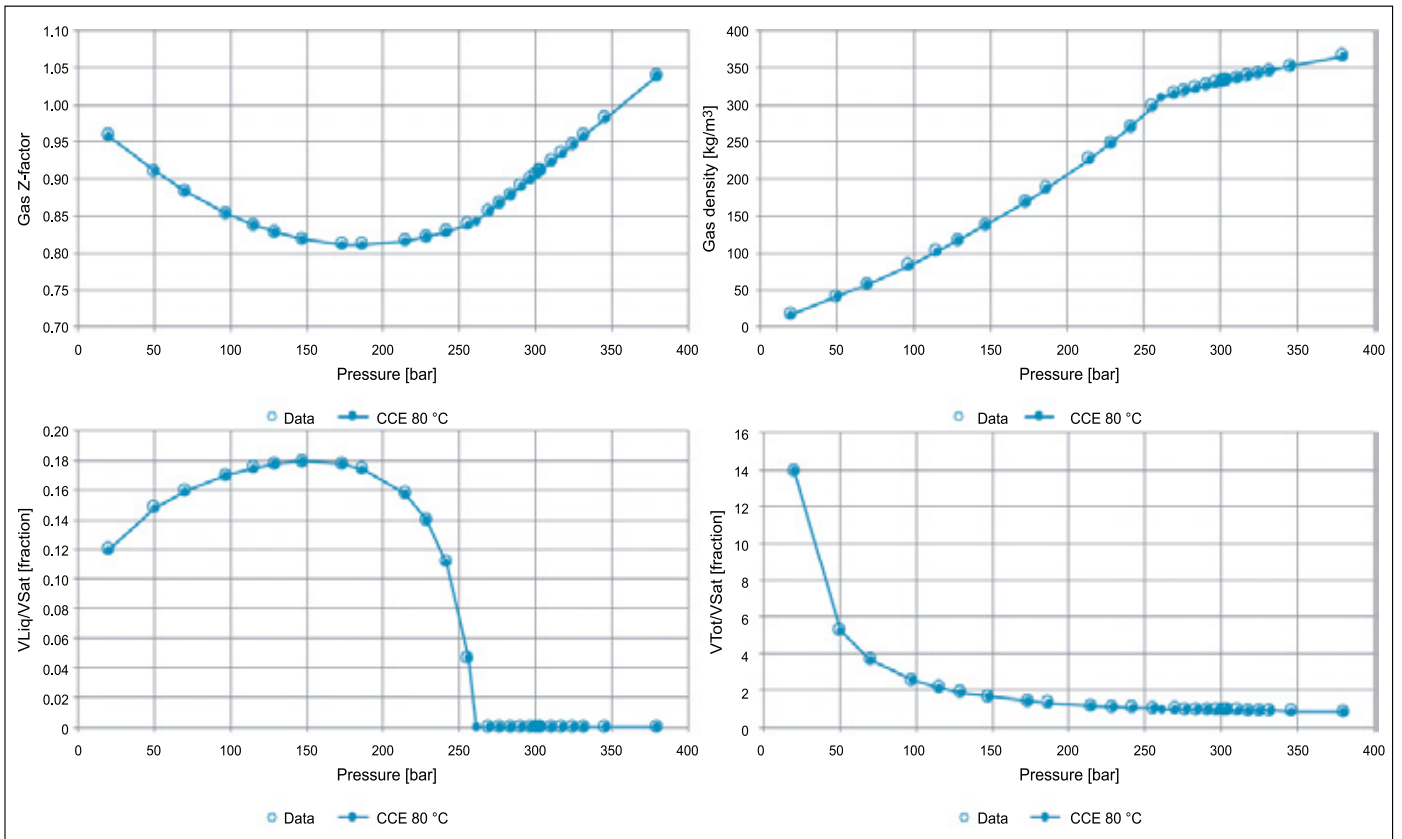


Figure 11. Calibration results for the CCE experiment vs observed data

Rysunek 11. Wyniki kalibracji dla badania CCE względem zaobserwowanych danych

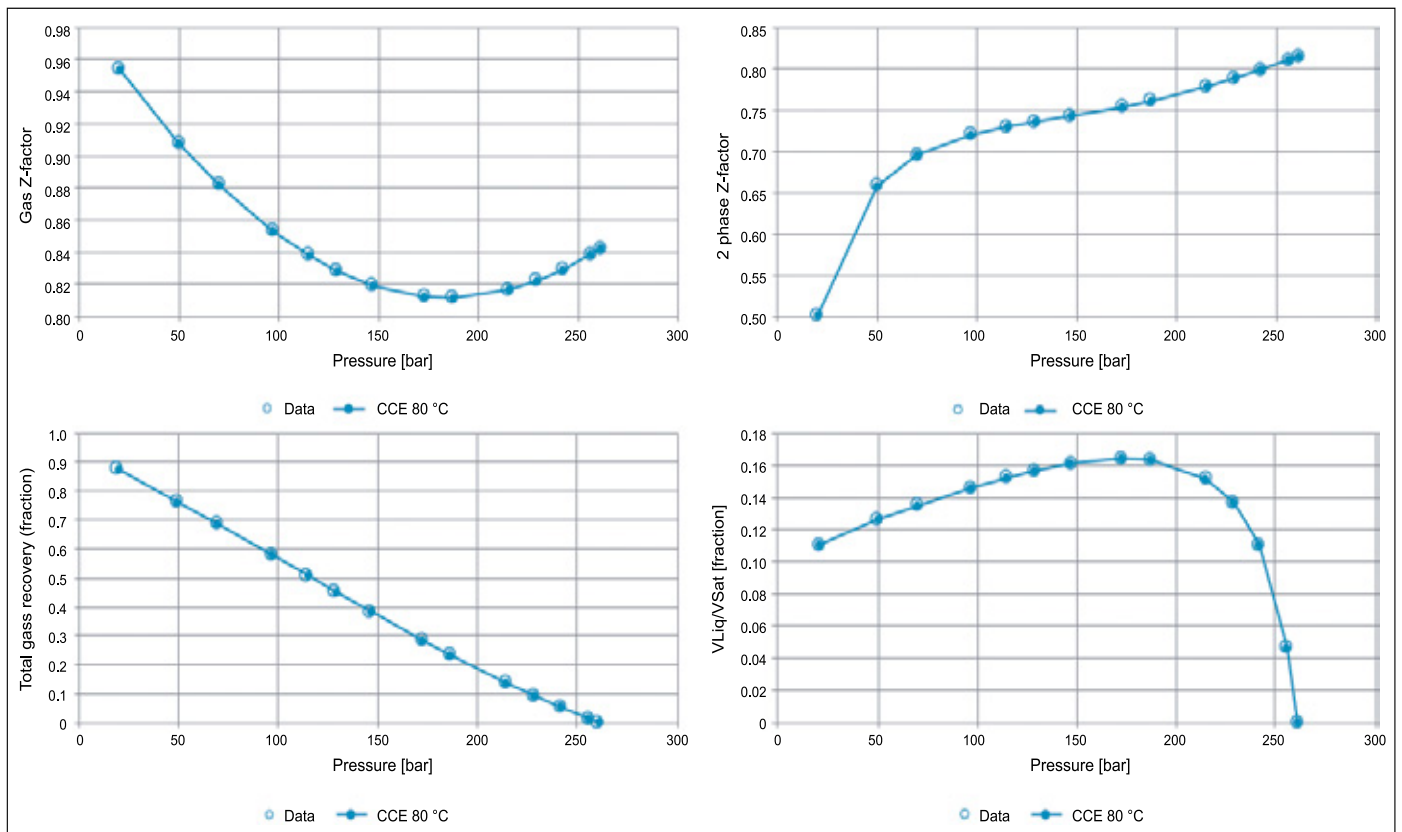


Figure 12. Calibration results for CVD experiment vs observed data

Rysunek 12. Wyniki kalibracji dla badania CVD względem zaobserwowanych danych

Table 2. Condensate composition

Tabela 2. Skład kondensatu

Component	[% mol]
N ₂	0.12
CO ₂	0.12
C1	21.16
C2	7.91
C3	5.97
i-C4–n-C5	7.52
C6–C8	16.74
C9–C10	18.27
C11–C14	14.55
C15–C19	6.49
C20+	1.14

Source: generated by authors

miscibility pressure for various (available) injection agents. The composition of the condensate is presented in Table 2. A comparison of the phase diagram for the initial reservoir fluid (reservoir fluid in the graph) and the phase diagram of the condensate is presented in Figure 13.

Based on the grouping recommendations for reducing the number of components and for constructing a ternary diagram, the groups created for the reservoir fluid are shown in Table 3.

The composition and phase diagram of the condensate dropped-out in the reservoir indicate a high content of ex-

pensive hydrocarbon components C6–C10. Xu et al. (2020) provides typical agents used for injection in gas condensate deposits. Their composition and the range of variation are shown in Table 4.

The composition of the injected fluid directly depends on its availability and ease of transportation or preparation. As a rule, gas extracted from the reservoir is used and mixed with a solvent in specific proportions, depending on the solvent’s availability. The agents of the following compositions were considered and summarized in Table 5.

Table 3. Components grouping for ternary diagrams

Tabela 3. Grupowanie składników dla diagramów trójskładnikowych

Component	Group
N ₂	(1)
CO ₂	(2)
C1	(1)
C2	(2)
C3	(2)
i-C4–n-C5	(2)
C6–C8	(3)
C9–C10	(3)
C11–C14	(3)
C15–C19	(3)
C20+	(3)

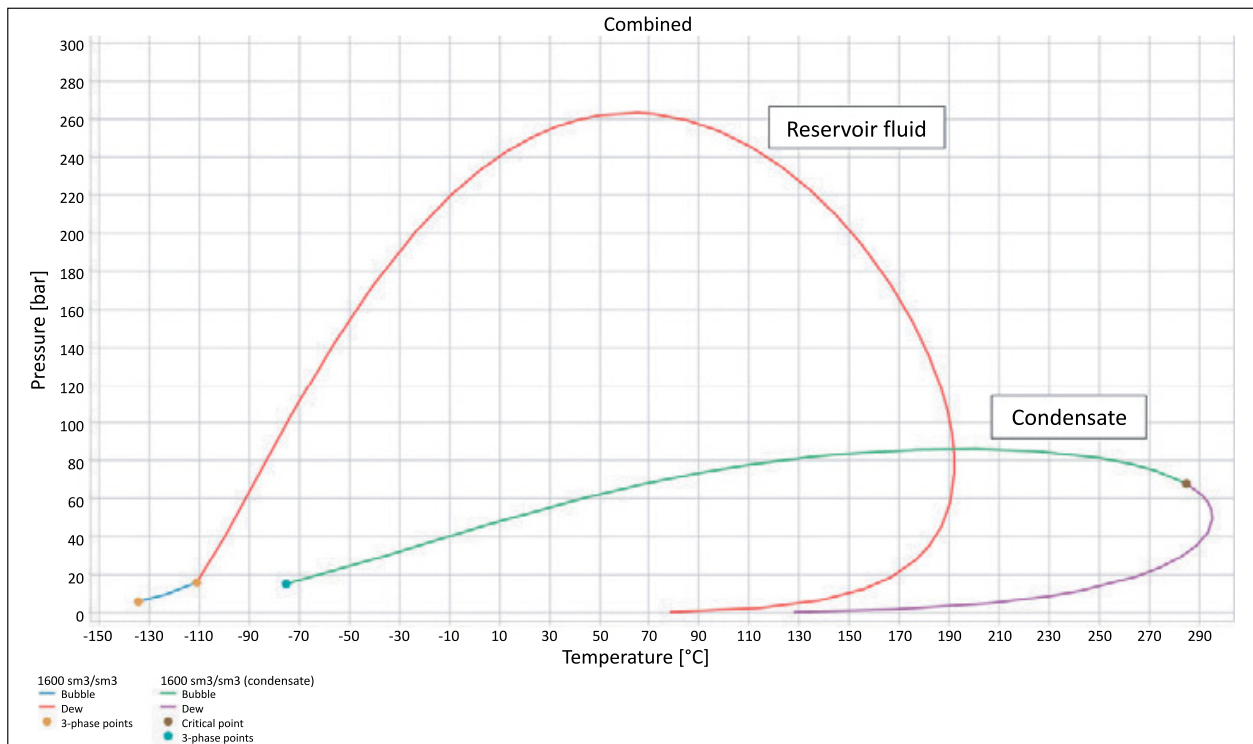


Figure 13. Phase envelopes for reservoir fluid and condensate (source: generated by authors)

Rysunek 13. Wykresy fazowe dla płynu złożowego i kondensatu (źródło: wygenerowane przez autorów)

Table 4. Typical composition of injected gas**Tabela 4.** Typowy skład zatłaczanego gazu

Component	CO ₂	Dry gas	Wet gas
N ₂	up to 2%	up to 2%	up to 2%
CO ₂	98%	up to 5%	up to 5%
C1	–	80–90%	65–75%
C2	–	1–5%	10–20%
C3	–	trace	1–10%
C4	–	trace	1–5%
C5	–	–	trace

Table 5. Typical composition of injected gas**Tabela 5.** Typowy skład wtryskiwanego gazu

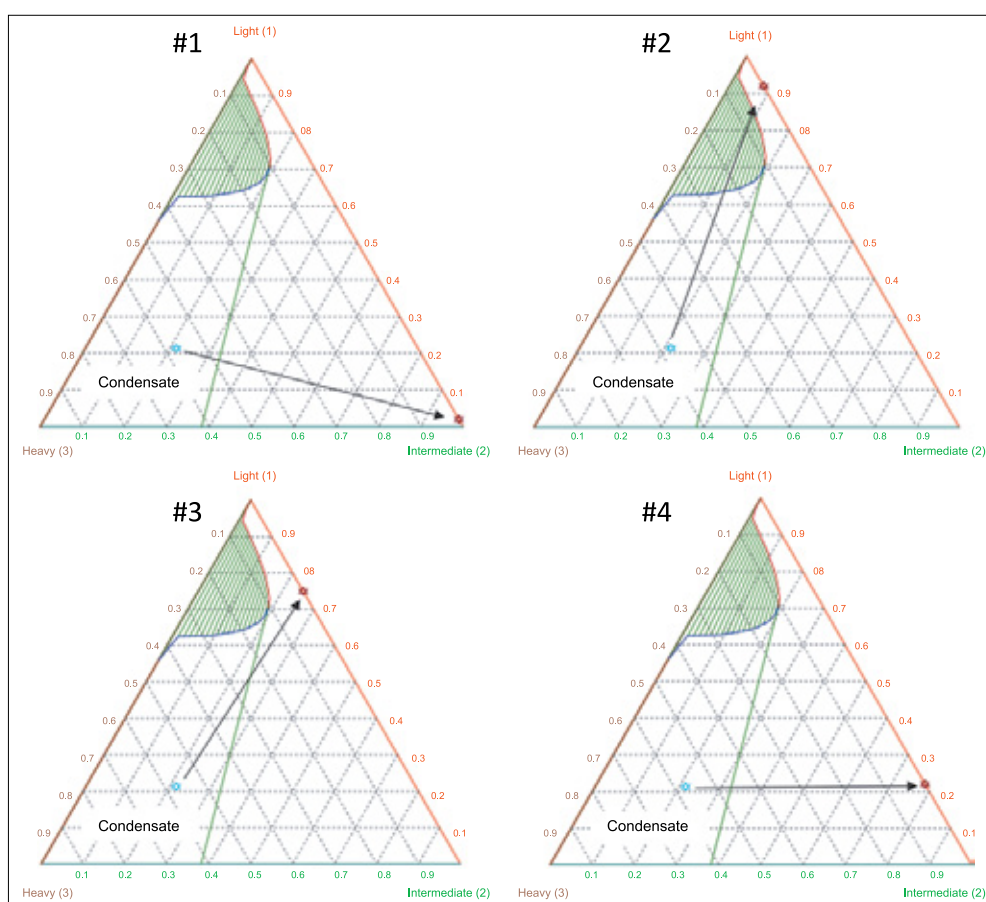
Component	Agent 1	Agent 2	Agent 3	Agent 4
	[%]			
N ₂	2	2	2	2
CO ₂	98	5	5	75
C1	–	90	73	20
C2	–	3	10	2
C3	–	–	8	1
C4	–	–	2	–

Table 6. Tested injection fluids**Tabela 6.** Testowane płyny do zatłaczania

Agent number	First contact MMP	Multi-contact MMP
	[bar]	
1	155.13	123.3
2	328.90	259.3
3	247.10	198.0
4	187.30	150.0

To estimate the minimum required miscibility pressure (MPP), the condensate composition and the mixtures from Table 5 were grouped, and a synthetic MMP experiment was conducted using the PVT package. The results of this synthetic experiment and the minimum required miscibility pressures are summarized in Table 6. Ternary visualization of mixtures 1–4 and the condensate at a pressure of 250 bar is shown in Figure 14.

Mixture #2, composed mainly of methane, is characterized by the highest value of the minimum required miscibility pressure (328 bar for first contact and 259 bar for multi-contact miscibility). Given the initial and current reservoir pressures, injection at these operating bottomhole pressures can lead to

**Figure 14.** Ternary diagrams for condensate and injection agents 1–4 at pressure 250 bars**Rysunek 14.** Diagramy trójskładnikowe dla kondensatu i środków zatłaczanych 1–4 przy ciśnieniu 250 barów

rock fracturing and simple gas circulation. In contrast, other mixtures have much lower minimum required miscibility pressures. Thus, the choice of agent depends on the ability to pressurize above the minimum required pressure, as well as on availability, transportation, and preparation of the agent. At an injection pressure of 250 bar, miscibility at the first contact is achievable for mixtures #1 and #4. However, it should be noted that the reservoir pressure will not increase instantaneously; therefore, miscibility at the first contact may only occur at the bottom of the injection well. In this case, a pilot project localized at the field level is recommended.

A pilot project can employ the huff-and-puff method, involving cycling production, injection, and pause before the next cycle. According to Sahai and Moghanloo (2022), laboratory studies are performed beforehand to determine the ratio of gas injected to displaced oil volume due to repeated huff-and-puff cycles at the core level. The optimal values of the periods and the possibility of achieving the minimum required miscibility pressure are also determined. The different number of days for a cycle and the length of the pause between injection and subsequent production were considered. The results showed that the efficiency depends on the size of the rock matrix sampled as a core. Efficiency increased with increasing sample size. The following sizes were considered: 0.01, 0.1, 1 and 10 m. The injection and production cycle was 30 days, and the pause between them varied from 1 to 90 days.

Dynamic reservoir model construction

To assess the impact of condensate dropped out from gas on the productivity of a horizontal well and to model miscible condensate displacement, a 3D hydrodynamic model was built. The compositional simulator Eclipse 300 was used to model fluid flow in the porous media. The simulator choice was based on the performance of industrial SPE reference cases and license availability. The simulated horizontal well H1 with 14 hydraulic fractures planes is shown in Figure 15.

Hydraulic fracturing in all simulation sensitivity cases was modeled using pseudo-connections. This method has been tested as alternative and easier approach compared to Local Grid Refinement (LGR), as noted in the publication by Lukin and Kondrat (2024). Pseudo-connections are generated for all cells penetrated by fracture planes, with connection factors modified based on fracture properties. For all sensitivity cases, similar fracture properties were used, summarized in Table 7: height (h), width (D_w), half length (X_f), and proppant permeability (K_{prop}).

The hydrodynamic model is based on an analogy to a tight gas condensate field located in the Dnieper Donetsk Depression.

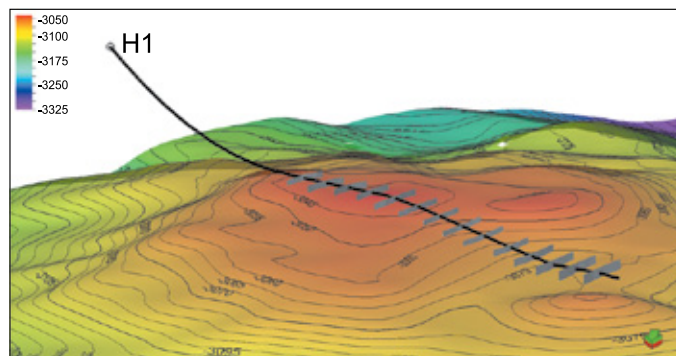


Figure 15. Well’s H1 trajectory and hydraulic fractures

Rysunek 15. Trajektoria odwiertu H1 i szczeliny hydrauliczne

Table 7. Fracture properties

Tabela 7. Właściwości szczeliny

h	D_w	X_f	K_{prop}
	[m]		[md]
15	0.03	75	1000

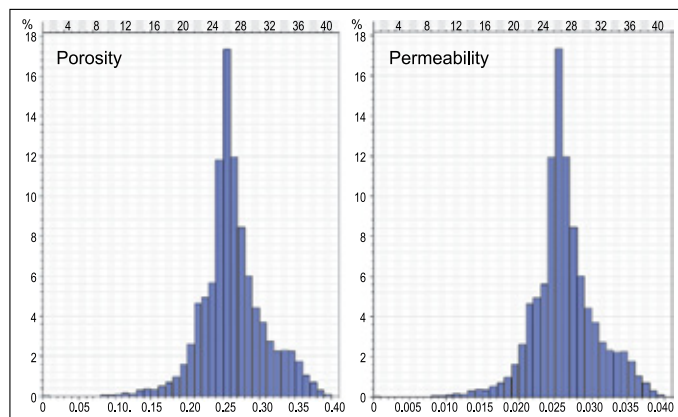


Figure 16. Distribution histograms for static model: porosity and permeability

Rysunek 16. Histogramy rozkładu dla modelu statycznego: porowatość i przepuszczalność

The reservoir is developed by well H1 and is characterized by low permeability, with an average permeability of 0.025 mD and average porosity of 0.25. Distribution histograms for porosity and permeability are presented in Figure 16. The property distribution is based on petrophysical interpretations of well logs and data analysis for major and minor variograms.

Unified relative permeability curves were used for the entire reservoir. End-point scaling was performed based on the porosity-water saturation relationship. Straight-line relative permeabilities were applied at the fracture level. The horizontal section of the well is 1440 m, with the distance between hydraulic fracturing stages of approximately 100 m. The simulation was performed with a downhole pressure limit for well H1 at around 50 bar for the baseline scenario. The

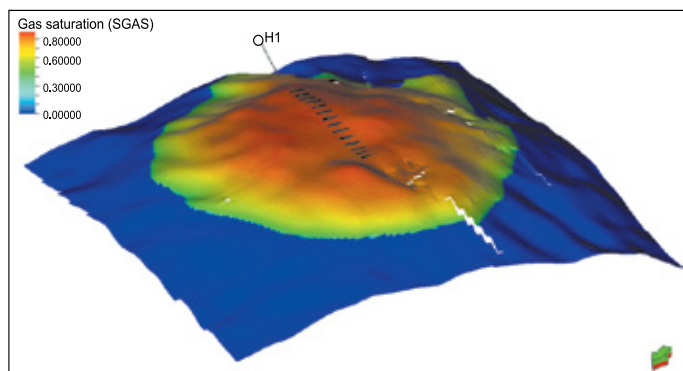


Figure 17. Water saturation distribution for hydrodynamic model with well H1 and 14 stages of hydraulic fractures

Rysunek 17. Rozkład nasycenia wodą dla modelu hydrodynamicznego z otworem H1 i 14 sekcjami szczelin hydraulicznych

initial pressure at the start of the simulation is 400 bar. The initial gas reserves after model initialization are 2.7 billion m^3 , and the initial condensate reserves are 1.05 million m^3 . The gas-water contact (GWC) is established at a depth of -3130 m. Figure 17 shows a hydrodynamic model, the horizontal well, and the 14-stage hydraulic fracturing.

The reservoir model consists of approximately 1 million cells, allowing for an acceptable CPU time of 1.5 hours. Gridding was performed with a lateral grid cell extension of $100 \text{ m} \times 100 \text{ m}$, while the vertical resolution is 0.5 m to capture vertical heterogeneity.

Simulation results

For the gas injection simulations, a 30-day injection and production cycle were used, with a 5-day pause between injection and subsequent production. The total simulation time for the pilot project is 11 months. Injection agents were chosen based on the recommendations of Xu et al. (2020) and Table 5. The pilot project was designed for 5 cycles, and the simulation was performed for mixtures No. 1–4. The results of the baseline scenario and huff-and-puff simulations with mixture No. 1 are shown below. The baseline case is characterized by depletion and is represented by a solid line in the figure below. As can be seen from Figure 18, the initial condensate flow rate is $180 \text{ m}^3/\text{day}$, which decreases sharply, reaching $2\text{--}3 \text{ m}^3/\text{day}$ within six months. No water production was observed in the stream.

Cumulative condensate production for the baseline scenario over 11 months is 3600 m^3 , while for the huff-and-puff scenario (mixture No. 1), it is 9000 m^3 . However, the advantage of using a compositional simulator lies in its ability to analyze production for each component separately. Figure 19 shows the production profiles for components C7–C8, C9–C10,

C11–C14, and C15–C19 for the baseline scenario (red line) and huff-and-puff (mixture 1 – green line). Additional condensate production in the second scenario is provided by components C7–C19, which are typically released in the reservoir after the pressure drops below the saturation pressure and remain stationary in the pore space.

Similar simulations were performed for mixtures 2–4. The resulting condensate production for all scenarios is shown in Figure 20. The cumulative condensate production for the pilot period for mixtures No. 2–4 is 6000 m^3 , 7900 m^3 , and 9120 m^3 , respectively.

Over the 11-month pilot project, the simulations showed a 2-fold increase in accumulated condensate production, and nearly 3-fold one for some mixtures. The condensate ring around well H1 for Baseline Scenario (2) and HnP Agent 4 (1) is presented in Figure 21. At the end of 11-month simulation period, the condensate ring was reduced by 110 m for the case with HnP Agent 4 compared to the baseline scenario.

The number of cycles for pilot projects can vary from 2 to 6, depending on the current reservoir pressure in the field. According to Haddad et al. (2023), such pilot projects aim to achieve 3 main goals:

- to test the feasibility of using huff-and-puff technology for a specific field or well;
- to estimate the maximum and optimal injectivity of wells;
- to confirm the miscibility of the agent with the reservoir fluid and determine the minimum required miscibility pressure.

Additionally, Haddad et al. (2023) noted that using this technology provides additional production not only through miscibility, but also through geomechanical processes, namely the reactivation of fractures formed due to multi-stage hydraulic fracturing when the injection pressure reaches or exceeds the fracture closing pressure.

It should also be noted that, in this paper, the procedure for determining the minimum required miscibility pressure during gas injection in low-permeability reservoirs was simplified. The work of Yang (2021) describes a more detailed approach to determining the miscibility pressure and systematizes methods proposed by various researchers. While most of them are theoretical, all of them have been tested for real fluid systems.

An important aspect not considered in this work is well injectivity. Xu et al. (2020) demonstrated the impact of the injection capacity for different wells (estimated using Hall plots) in a real case study. Each proposed injection mixture has a different viscosity, meaning that at the same bottom-hole injection pressures, the volume of the injected agent will vary. In the scenarios proposed in this paper, injection wells were constrained by the maximum allowable BHP, and well injectivity (agent injection volume) was controlled by the properties of the

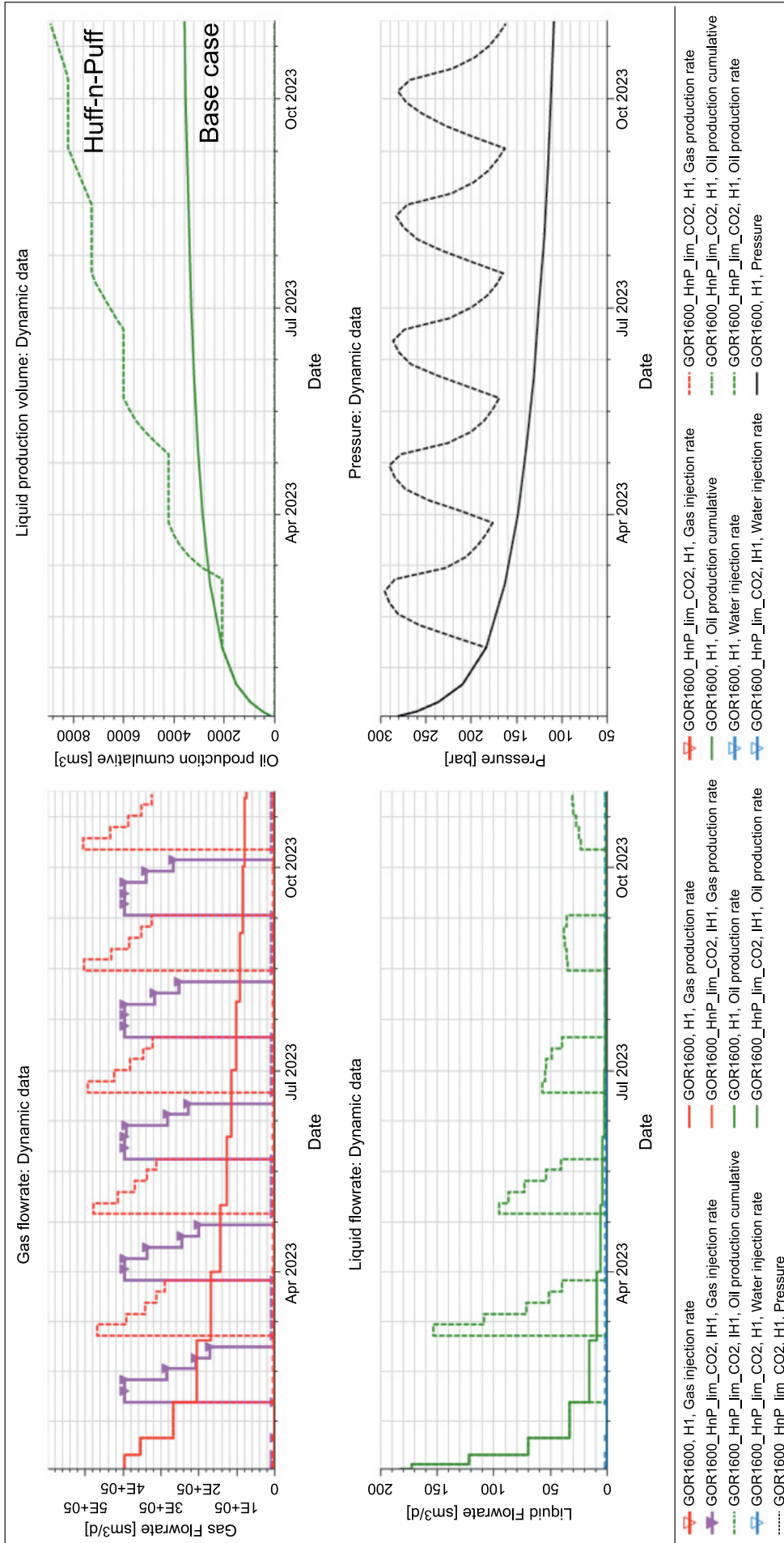


Figure 18. Production/injection profiles for base and huff-and-puff (agent 1) scenarios
Rysunek 18. Profile eksploatacji/zatlaczania dla scenariusza *huff-and-puff* (czynnik 1)

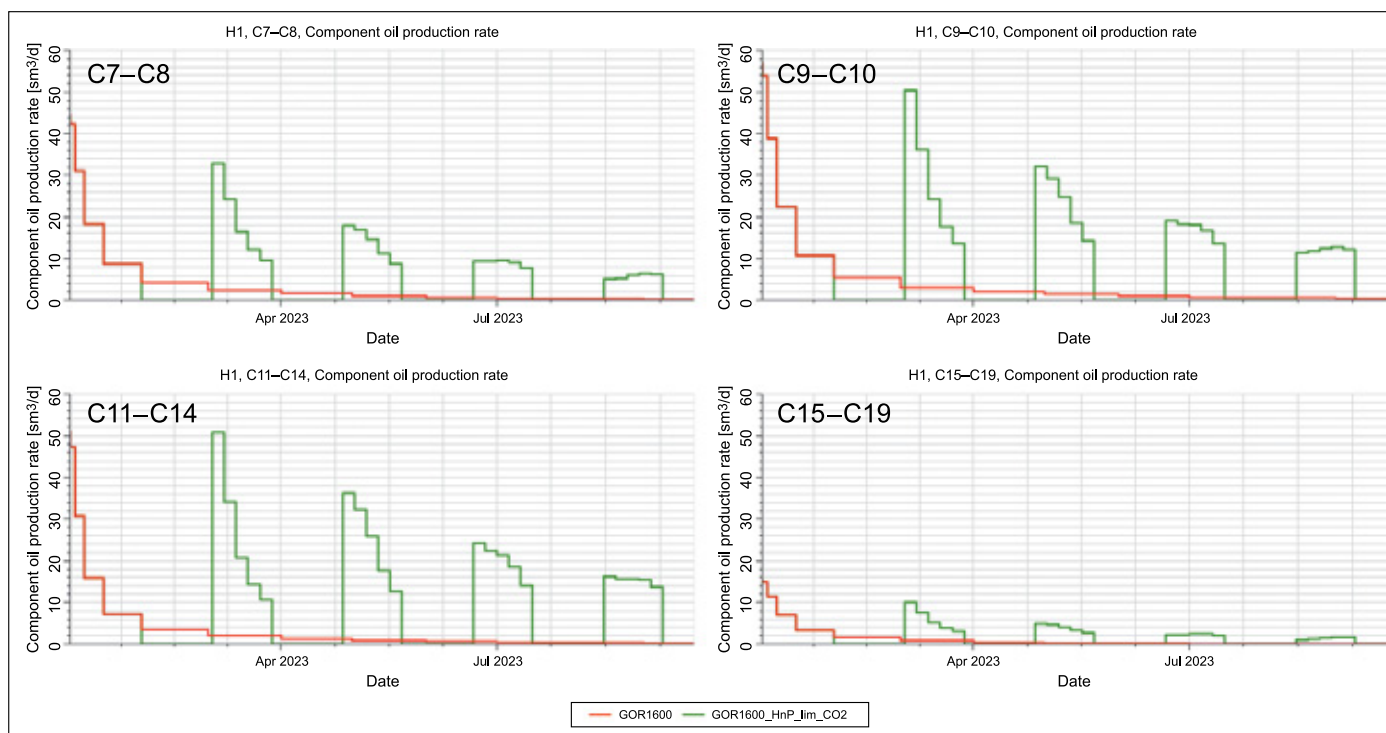


Figure 19. Component production profiles for base and huff-and-puff (agent 1) scenarios

Rysunek 19. Profile eksploatacji komponentów dla scenariusza podstawowego i scenariusza *huff-and-puff* (czynniki 1)

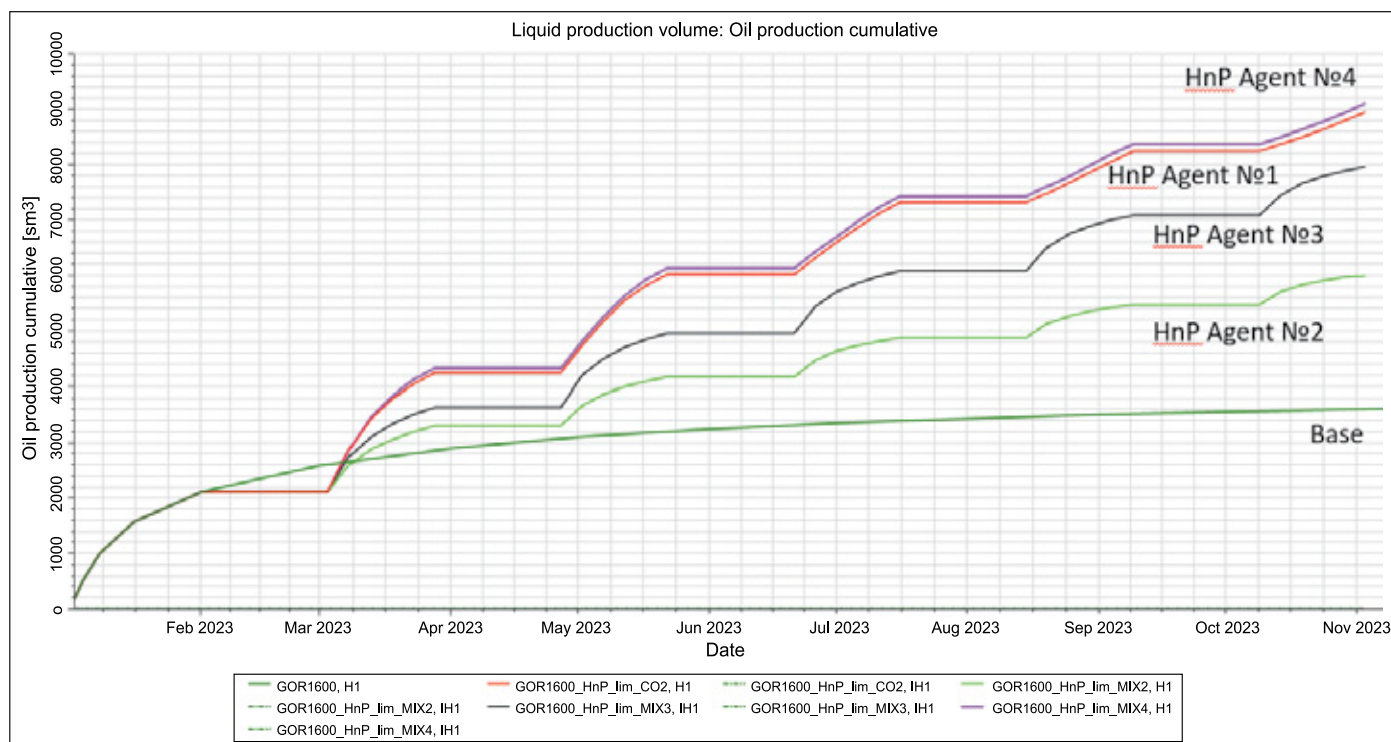


Figure 20. Cumulative condensate production for base and huff-and-puff (agents 1–4) scenarios

Rysunek 20. Łączna produkcja kondensatu dla scenariusza podstawowego i scenariusza *huff-and-puff* (czynniki 1–4)

mixtures, calculated using the equation of state based on their composition. However, any decision regarding the implementation of a pilot project must be supported by laboratory tests and the availability of injection agents. The relevance of CO₂

injection for the combined purpose of increasing condensate recovery and CO₂ utilization was considered by Burachok et al. (2021), where 100% CO₂ injection was designed for a depleted gas condensate field. However, to implement such a project,

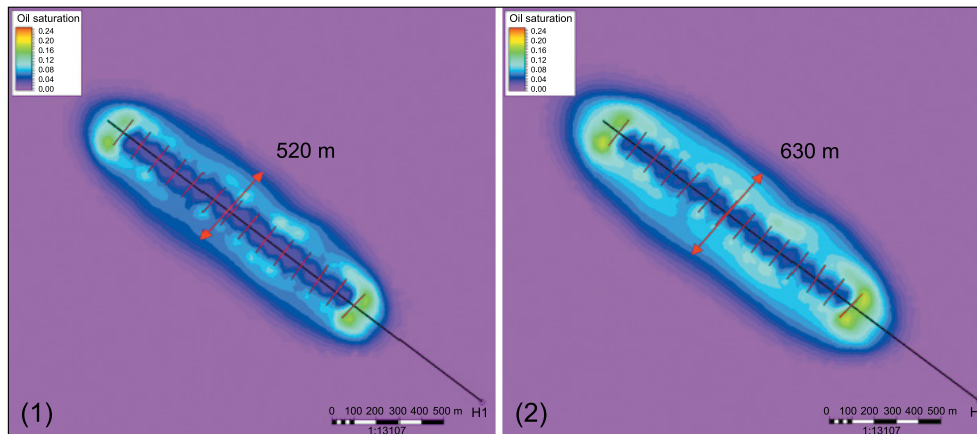


Figure 21. Condensate saturation around well H1 for HnP Agent 4 (1) and Baseline Scenario (2)

Rysunek 21. Nasylenie kondensatem wokół odwiertu H1 dla czynnika HnP 4 (1) i scenariusza odniesienia (2)

it is necessary to consider the risks of CO₂ migration in the reservoir, especially if this method of increasing condensate recovery is designed for a reservoir with wells that have been subjected to multi-stage hydraulic fracturing.

Conclusions

Maximizing hydrocarbon recovery in gas condensate reservoirs can be achieved by maintaining pressure above the dew point, which prevents condensate drop out in the reservoir. However, in the case of tight formations with horizontal wells and multi-stage hydraulic fracturing, the pressure drop around the well is significantly higher compared to conventional reservoir, making it impossible to maintain pressure above saturation pressure. Additionally, there are reservoirs with fluids characterized by a dew point pressure very close to the initial reservoir pressure. Most gas condensate fields in Ukraine are already mature and depleted; under these conditions, pressure maintenance using agents that are not miscible with the reservoir fluid will not result in additional recovery from injection projects.

A systematic method for selecting gas composition for injection during the equation of state modeling process was presented. This includes ternary visualization and determining the minimum required miscibility pressure to form a single-phase flow in the reservoir. The formation of a condensate ring significantly reduces well productivity by blocking part of the pore space and reducing the relative phase permeability of gas in the presence of liquid due to two-phase flow formation. Since the condensate dropping out in the reservoir contains valuable hydrocarbon components, its loss worsens the economic performance.

Using a specific example of reservoir fluid, a method for assessing the composition of condensate precipitated in the

reservoir using a PVT package and a compositional hydrodynamic model was tested. A technology for selecting a mixing agent to vaporize and subsequently mobilize condensate was simulated. The simulation results showed that a mixture of hydrocarbon gas with a solvent in the form of CO₂ is characterized by the lowest required minimum miscibility pressure (MMP) – 123.3 bar (Agent #1), while dry gas has the highest MMP – 259 bar (Agent #2). A detailed description of the huff-and-puff technology using a hydrodynamic simulator makes it possible to test the results of the PVT study and determine whether miscibility can actually be achieved in the reservoir. Validation was also performed by checking the residual condensate saturation behind the displacement front when the injection pressure and reservoir pressure exceeded the required minimum miscibility pressure.

The cumulative condensate production over the 11-month pilot period while injecting the agents was as follows: Agent 2 – 6000 sm³, Agent 3 – 7900 sm³, Agent 1 – 9000 sm³, Agent 4 – 9120 sm³. The condensate bank around well H1 is reduced by 110 m compared to the baseline scenario when using HnP Agent 4. Injection agents selected based on minimum miscibility pressure values via the PVT package resulted in the highest cumulative condensate production over the 11-month huff-and-puff simulation. This methodology involves prior Equation of state generation to estimate condensate composition at specific pressures during PVT experiments.

The described methodology is relevant for all gas condensate fluid systems and can be used by reservoir engineers to optimize the development of low-permeability gas condensate reservoirs. Future areas of this work include testing this methodology on a larger number of fluids, optimizing the design of multi-stage hydraulic fracturing by explicit fractures modeling, accounting for the direction of minimum stress, fracturing pressure gradients, and the selection of fracturing fluids and proppants.

References

- Al Kharusi M., Cobanoglu M., Al Shukri M., Al Bulushi S., 2019. Challenges and Modeling Results of a Mature Rich Gas Condensate Field Redevelopment Study Applying Depletion and Multiple EOR Methods to Unlock Field Potential. *International Petroleum Exhibition & Conference, Abu Dhabi, UAE*. DOI: 10.2118/197475-MS.
- Bang V., Yuan C., Pope G., Sharma M., Baran Jr. J., Skildum J., Linnemeyer H., 2008. Improving Productivity of Hydraulically Fractured Gas Condensate Wells by Chemical Treatment. *Offshore Technology Conference, Houston, Texas, USA*. DOI: 10.4043/19599-MS.
- Burachok O., Kondrat O., Matkivskyi S., Pershyn D., 2021. Comparative Evaluation of Gas-Condensate Enhanced Recovery Methods for Deep Ukrainian Reservoirs: Synthetic Case Study. *SPE Europec featured at 82nd EAGE Conference and Exhibition*. DOI: 10.2118/205149-MS.
- Ghiri M.N., Nasriani H.R., Sinaei M., Najibi S.H., Nasriani E., Parchami H., 2015. Gas Injection for Enhancement of Condensate Recovery in a Gas Condensate Reservoir. *Energy Sources. Part A: Recovery, Utilization and Environmental Effects*, 37(8): 799–806. DOI: 10.1080/15567036.2011.596901.
- Haddad D.E., Long H., Agrawal R., Kumar H.T., 2023. Reservoir Mechanisms of Unconventional Gas Injection EOR; Insights from Field Trials in the Eagle Ford. *SPE/AAPG/SEG Unconventional Resources Technology Conference, Denver, Colorado*. DOI: 10.15530/urtec-2023-3862004.
- Hamdi H., Clarkson C.R., Esmail A., Sousa M.C., 2020. Importance of multiple-contact and swelling tests for huff-n-puff simulations: A montney shale example. *Proceedings – SPE Annual Technical Conference and Exhibition*. DOI: 10.2118/201557-MS.
- Lukin O., Kondrat O., 2024. Utilizing well-reservoir pseudo-connections for multi-stage hydraulic fracturing modeling in tight gas saturated formation. *Mining of Mineral Deposits*, 18(2): 113–121. DOI: 10.33271/mining18.02.113.
- Mohammed N., Abbas A.J., Enyi G.C., Suleiman S.M., Edem D.E., Abba M.K., 2020. Alternating N₂ gas injection as a potential technique for enhanced gas recovery and CO₂ storage in consolidated rocks: an experimental study. *Journal of Petroleum Exploration and Production Technology*, 10(8): 3883–3903. DOI: 10.2118/202716-MS.
- Pope G., Wu W., Narayanaswamy G., Delshad M., Sharma M., Wang P., 2000. Modeling Relative Permeability Effects in Gas-Condensate Reservoirs With a New Trapping Model. *SPE Reservoir Evaluation and Engineering*, 3(02): 171–178. DOI: 10.2118/62497-PA.
- Rivero J.A., Faskhoodi M., Ferrer G.G., Mukisa H., Zhmodik A., 2019. Huff-and-Puff Enhanced Oil Recovery in the Liquids-Rich Portion of the Montney: Applications for Gas Condensates. *SPE/AAPG/SEG Unconventional Resources Technology Conference, Denver, Colorado, USA*. DOI: 10.15530/urtec-2019-979.
- Sahai R., Moghanloo R.G., 2022. Impact of Soaking Time on the Efficacy of Miscible Gas Injection into Hydraulically Fractured Shale Wells. *SPE/AAPG/SEG Unconventional Resources Technology Conference*. DOI: 10.15530/urtec-2022-3724055.
- Seteyeobot I., Jamiolahmady M., Jaeger P., Nasieef A., 2021. An Experimental Study of the Effects of CO₂ Injection on Gas/Condensate Recovery and CO₂ Storage in Gas-Condensate Reservoirs. *SPE Annual Technical Conference and Exhibition*. DOI: 10.2118/206117-MS.
- Stalkup Jr. F.I., 1983. Miscible displacement. *Society of Petroleum Engineers Monograph series, Dallas, series 8*.
- Weisstein E.W. Ternary Diagram. <<https://mathworld.wolfram.com/TernaryDiagram.html>> (access: 05.06.2021).
- Xu S., BinAmro A.A., Mabrook M., 2020. Miscible Gas Injection EOR, Carbonate Reservoirs Well Injectivity Field Cases. *International Petroleum Exhibition & Conference, Abu Dhabi, UAE*. DOI: 10.2118/202720-MS.
- Yang G., 2021. Minimum Miscibility Pressure of Gas Injection in Unconventional Reservoirs. *SPE Annual Technical Conference and Exhibition, Dubai, UAE*. DOI: 10.2118/208625-STU.



Prof. Oleksandr KONDRAT, Sc.D.
Professor at the Department of Oil and Gas
Production
Vice-Rector of the Ivano-Frankivsk National
Technical University of Oil and Gas
15 Karpatska Str., Ivano-Frankivsk, Ukraine 76019
E-mail: oleksandr.kondrat@nung.edu.ua



Oleh LUKIN, M.Sc.
Doctoral Student at the Department of Oil and Gas
Production
Ivano-Frankivsk National Technical University of Oil
and Gas
15 Karpatska Str., Ivano-Frankivsk, Ukraine 76019
E-mail: oleh.lukin@nung.edu.ua